1-1-2011

Energy Deposition in the Breast During CT Scanning: Quantification and Implications for Dose Reduction

Franco Rupcich
Marquette University

Iacovos Kyprianou
US Food and Drug Administration

Andreu Badal
US Food and Drug Administration

Taly Gilat Schmidt
Marquette University, tal.gilat-schmidt@marquette.edu

Energy deposition in the breast during CT scanning: quantification and implications for dose reduction

Franco Rupcich[a], Iacovos Kyprianou[b], Andreu Badal[b], Taly Gilat Schmidt[a]
[a]Dept. of BME Marquette University, 1515 W. Wisconsin Ave., Milwaukee, WI, USA 53201-1881;
[b]Division of Imaging and Applied Mathematics (OSEL/CDRH), US Food and Drug Administration, 10903 New Hampshire Ave, Silver Spring, MD, 20993-0002

ABSTRACT

Studies suggest that dose to the breast leads to a higher lifetime attributable cancer incidence risk from a chest CT scan for women compared to men. Numerous methods have been proposed for reducing dose to the breast during CT scanning, including bismuth shielding, tube current modulation, partial-angular scanning, and reduced kVp. These methods differ in how they alter the spectrum and fluence across projection angle. This study used Monte Carlo CT simulations of a voxelized female phantom to investigate the energy (dose) deposition in the breast as a function of both photon energy and projection angle. The resulting dose deposition matrix was then used to investigate several questions regarding dose reduction to the breast: (1) Which photon energies deposit the most dose in the breast, (2) How does increased filtration compare to tube current reduction in reducing breast dose, and (3) Do reduced kVp scans reduce dose to breast, and if so, by what mechanism? The results demonstrate that while high-energy photons deposit more dose per emitted photon, the low-energy photons deposit more dose to the breast for a 120 kVp acquisition. The results also demonstrate that decreasing the tube current for the AP views to match the fluence exiting a shield deposits nearly the same dose to the breast as when using a shield (within ~1%). Finally, results suggest that the dose reduction observed during lower kVp scans is caused by reduced photon fluence rather than the elimination of high-energy photons from the beam. Overall, understanding the mechanisms of dose deposition in the breast as a function of photon energy and projection angle enables comparisons of dose reduction methods and facilitates further development of optimized dose reduction schemes.

Keywords: Dose, Monte Carlo simulation, dose reduction, CT, dose deposition matrix

1. INTRODUCTION

It has been estimated that over 46 million CT scans are performed each year in the United States[1]. While these scans can be crucial in diagnosing disease, they impart higher levels of radiation dose compared to other conventional x-ray imaging procedures[2]. Although no large-scale epidemiological study has reported specific levels of cancer risk associated with CT scans, the risk of cancer incidence from these scans has been estimated from atomic bomb survivors. The Biological Effects of Ionizing Radiation (BEIR) VII Phase 2 report on *Health Risks from Exposure to Low Levels of Ionizing Radiation* reports that women exposed to radiation at any age suffer a higher lifetime attributable risk (LAR) of cancer induction and mortality than men exposed at the same age[3]. This phenomenon is observed even when breast, ovarian, and uterine cancers are excluded.

Many groups have evaluated methods of reducing dose to radiosensitive organs such as the breast, including bismuth shielding, reduced kVp, and tube-current modulated scans.[4,5,6,7,8] These methods differ in how they alter the spectrum and fluence across projection angle. For example, bismuth shielding removes a higher fraction of low-energy photons from the beam, while reduced kVp eliminates high-energy photons from the beam. While low-energy photons are more likely to be absorbed where the beam enters the patient, such as in the breast during AP views, high-energy photons deposit more dose per interaction.

This study aims to quantify the underlying causes of dose reduction in previously proposed methods in order to facilitate effective application and development of optimized dose reduction schemes. Monte Carlo simulations of a voxelized female phantom were used to create a normalized dose deposition matrix, quantifying the dose to the breast per photon emitted from the source as a function of both x-ray energy and view angle. This matrix was then used to investigate several questions regarding dose reduction to the breast: 1) which photon energies deposit the most dose to the breast in a conventional CT scan; 2) how does the reduction in dose due to preferential filtering of low energy photons (bismuth

Medical Imaging 2011: Physics of Medical Imaging, edited by Norbert J. Pelc, Ehsan Samei, Robert M. Nishikawa,
Proc. of SPIE Vol. 7961, 796128 · © 2011 SPIE · CCC code: 1605-7422/11/$18 · doi: 10.1117/12.878861

shields) compare to reduced fluence across all energies (angularly-dependent tube current reduction); and 3) do reduced kVp scans reduce dose to breast, and if so, by what mechanism?

2. MATERIALS AND METHODS

2.1 Monte Carlo Simulations

All x-ray projections and CT simulations were performed using the penEasy software package,[9,10] which relies on the PENELOPE Monte Carlo radiation transport routines[11].

2.2 Patient Phantom

This study used the voxelized anthropomorphic 26-year-old female phantom, Ella, from the Virtual Family[12]. The phantom was cropped to the thorax, measuring 31 cm by 22 cm in the lateral and anteroposterior directions, respectively, and 30 cm in the axial direction. Voxels representing breast material were modeled as 100% glandular tissue and were surrounded by a thick layer of adipose voxels. Voxels representing muscle, soft tissue, bone, cartilage, fat, blood, skin, and red bone marrow were all comprised of their respective tissue-equivalent materials.[13,14,15]

2.3 Generating X-ray Spectra

The 80 and 120 kVp polyenergetic x-ray spectra used in this study were generated using SPEC78[16] assuming a tungsten target, 12° anode angle, 0% voltage ripple, and 6-mm aluminum filtration. The resulting spectra were convolved with a 3-point boxcar kernel, down-sampled from dE = 0.5 keV to 1 keV, and normalized to have a sum of one. The down-sampling was performed to reduce the computation time during simulations.

2.4 Energy Deposition Simulations

The transport of monoenergetic photons through the voxelized female phantoms were simulated at 5 – 150 keV in 1 keV increments at 360 projections in 1 degree increments. We chose to perform monoenergetic simulations so that we could investigate the effects of specific energy levels on dose. The source-to-detector distance for each simulation was 100 cm, with a source-to-isocenter distance of 50 cm. The lateral and axial extents of the detector were 100 cm and 16 cm respectively, while the detector pixel resolution was 0.25 mm. For each photon energy at each projection angle, ten million photons were tracked, and the energy deposited in the breast tissue was tallied. Bowtie filtration was not simulated. The system geometry is diagrammed in Figure 1.

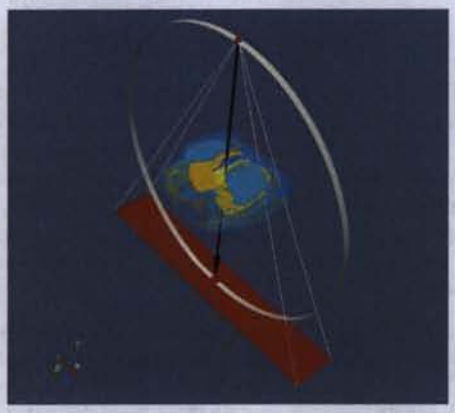

Figure 1: Scan geometry. The thorax was cropped to 31 cm by 22 cm in the lateral and anteroposterior directions, respectively, and 30 cm in the axial direction. The first view angle of the scan is AP (arrow). The detector measures 100 cm laterally 16 cm axially (rectangle).

2.5 Dose Calculations

The energy deposition to the breast, reported in eV per photon emitted from the source, was converted to dose to breast by first converting eV to Joules and then dividing by the total mass of breast tissue, resulting in the *normalized dose deposition matrix, $Q(\theta,E)$*, quantifying the dose in the breast per photon emitted from the source (mGy/photon) for each energy level, E, and projection angle, θ, for a scan with the abovementioned geometry consisting of 360 views.

A dose deposition matrix, $D(\theta,E)$, quantifying the dose to the breast (mGy as opposed to mGy/photon) at each energy level and projection angle for a specified spectrum and number of photons, can be calculated using the normalized dose deposition matrix as described in Equation 1,

$$D(\theta,E) = N(\theta)\cdot\Phi(\theta,E)\cdot Q(\theta,E) \quad (1)$$

where $N(\theta)$ is the number of photons emitted from the source at view angle, θ; $\Phi(\theta,E)$ is the probability of a photon emitted at angle, θ, and energy, E (i.e. a normalized input spectrum for view angle θ); and $Q(\theta,E)$ is the normalized dose deposition matrix (i.e., dose to breast per photon at angle, θ, and energy, E). The total dose to breast for a scan, D_{Total}, can be calculated by summing the dose deposition matrix over angle and energy, as described in Equation 2.

$$D_{Total} = \sum_{\theta} N(\theta)\sum_{E}\Phi(\theta,E)Q(\theta,E) = \sum_{\theta}\sum_{E} D(\theta,E) \quad (2)$$

Note that the normalized dose deposition matrix, Q, is the output of a Monte Carlo simulation for a specific CT geometry, while N and Φ are user-modifiable parameters. Together, N and Φ represent an input x-ray spectrum. Modifying these two parameters allows for calculating total dose for various acquisition methods and scan parameters. For example, increasing or decreasing N is equivalent to an increase or decrease in the tube-current (since tube-current dictates the number of photons emitted from the source). Thus N can be used to control the tube current and to model acquisitions in which tube-current varies across view angle. Note that setting N to zero at desired angles represents partial-angle scanning. Similarly, spectra filtration and kVp levels can be changed by properly modifying both N and Φ.

The normalized dose deposition matrix, $Q(\theta,E)$, was used along with parameters $N(\theta)$ and $\Phi(\theta,E)$ to calculate a dose deposition matrix, $D(\theta,E)$, for each of the studied scan methods described in Section 2.7.

2.6 Validation

To validate the method of calculating total dose to the breast described in Section 2.5, we performed a Monte Carlo simulation consisting of 360 views, one billion photons per view, and a 120 kVp polyenergetic spectrum generated via SPEC78. The scan geometry was identical to that used to generate the normalized dose deposition matrix, Q, described in Section 2.4. The total dose to breast tissue output from this simulation was compared to that calculated using Equation 2 assuming the 120 kVp spectrum and one billion photons per view. We performed a similar validation using the 80 kVp spectrum.

2.7 Investigation of Dose Reduction Methods

We investigated several dose reduction techniques to better understand the underlying mechanisms behind their respective dose savings. A 120 kVp scan was used both as a reference and to determine the photon energies that deposit the most dose to the breast. We also performed calculations to quantify the dose reduction effects of shielding compared to an equivalent reduction in emitted photon fluence for the AP views. Finally, to investigate the effects of lower kVp on dose reduction, we compared 80 kVp scans at the same number of emitted photons as the reference 120 kVp scan and with the number of emitted photons adjusted to deposit the same dose to the detector as the reference scan.

2.7.1 Reference Scan

To quantify which photon energies deposit the most dose to the breast in a conventional CT scan, the dose deposition matrix, $D(\theta,E)$, was calculated using Equation 1, with $\Phi(\theta,E)$ equal to the normalized 120 kVp spectrum, $\Phi_{120}(E)$, (Figure 2) for all θ. Since we are interested only in relative dose reduction, the absolute number of photons used in Equation 1 is irrelevant. Therefore, we set the number of photons per view, $N(\theta)$, equal to one for all angles. The total dose for the reference scan was calculated using Equation 2.

2.7.2 Breast Shielding and Tube Current Reduction

Using the normalized dose deposition matrix, we estimate the dose reduction effects of a shield by modeling the spectrum that exits a typical bismuth breast shield (0.06 mm lead equivalent) for the 130 degrees of view angles centered on the AP view. The shield-filtered spectrum, $\Phi_{shield}(E)$, was determined by calculating the transmission of the normalized 120 kVp spectrum, $\Phi_{120}(E)$, through the 0.06 mm lead[4] (Figure 2). The shield-filtered spectrum, $\Phi_{shield}(E)$, was not re-normalized, and so it accounted for the spectral shape due to both the preferential filtering of low energies and the overall reduction in photons exiting the shield. The dose deposition matrix, $D(\theta,E)$, was then calculated using

Equation 1, with $N(\theta)$ equal to one. For the 130 AP angles centered about the AP view, $\Phi(\theta,E)$ was equal to $\Phi_{shield}(E)$. For the remaining 230 angles, $\Phi(\theta,E)$ was equal to the conventional 120 kVp spectrum, $\Phi_{120}(E)$. The total dose for the shield scan was calculated using Equation 2.

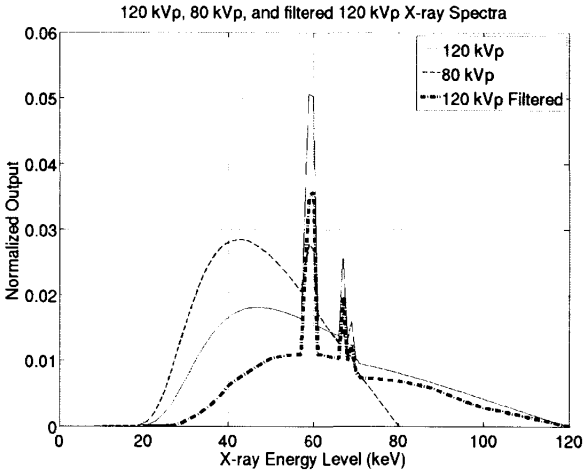

Figure 2 120kVp (solid), 80 kVp (dashed) and 120 kVp filtered through 0.06 mm lead (thick dot-dash) spectra

As seen in Figure 2, breast shields reduce the number of photons at all energies, with the greatest reduction of photons at low energies. To understand the dose reduction effects of the filtration of low energies compared to the overall reduction in photons, the dose deposition matrix, $D(\theta,E)$, was calculated using Equation 1 with $\Phi(\theta,E)$ equal to the typical 120 kVp spectrum, $\Phi_{120}(E)$, for all angles, but with the tube-current reduced for the 130 degrees of AP views to match the number of photons exiting the shield. The sum of the shield-filtered spectrum, $\Phi_{shield}(E)$, over energy, was equal to 0.6065. Therefore, $N(\theta)$ was set equal to 0.6065 for the 130 degrees of views centered at the AP view and to one for the remaining 230 angles.. The total dose was calculated using Equation 2.

2.7.3 Reduced kVp Scans

The purpose of the following two protocols was to investigate the effects of lower kVp scans on dose reduction, and to determine if any observed reduction in dose to the breast is caused by the elimination of high-energy photons from the spectrum. In this study, we do not consider the increased contrast at lower kVp for certain materials.

The dose deposition matrix, $D(\theta,E)$, was calculated for an 80 kVp scan using Equation 1, with $\Phi(\theta,E)$ equal to $\Phi_{80}(E)$ (Figure 2) for all θ, and with $N(\theta)$ equal to one. In this case, the number of photons exiting the source in the 80 kVp scan is equal to that in the 120 kVp scan. The total dose for this scan was calculated using Equation 2.

We performed a second calculation with the number of photons in the 80 kVp scan increased to provide equivalent dose to the detector as the 120 kVp scan. This case is expected to provide similar noise variance between 120 kVp and 80 kVp scans. The factor, α, by which to increase the number of photons in the 80 kVp scan, was calculated using Equation 3,

$$\alpha = \frac{S_{120}}{S_{80}} \tag{3}$$

where S_{120} and S_{80} were the signals at the detector (estimated by Monte Carlo simulation) for an AP projection of the voxelized phantom for a 120 kVp and an 80 kVp spectrum, respectively. We calculated α to be 1.3. The dose deposition matrix, $D(\theta,E)$, was calculated for an 80 kVp scan using Equation 1, with $N(\theta)$ equal to 1.3, and $\Phi(\theta,E)$ equal to a normalized 80 kVp spectrum, $\Phi_{80}(E)$, (Figure 2), for all θ. The total dose for the reduced kVp scan was calculated using Equation 2.

3. RESULTS

3.1 Validation Results

The percent difference between total dose to breast from the 120 kVp polyenergetic Monte Carlo simulation and that calculated using Equation 2 was 0.06%. Similarly, the percent difference for the 80 kVp scan was 0.11%.

3.2 Dose Results

Figure 3a shows the normalized dose-deposition matrix, $Q(\theta,E)$, while Figure 3b shows the dose deposition matrix, $D(\theta,E)$, for a reference scan of 120 kVp. $Q(\theta,E)$ quantifies the dose per incident photon, while $D(\theta,E)$ accounts for the different number of photons at each incident energy of a 120 kVp scan. Note that the relatively high dose peaks in (b) at approximately 60, 67, and 69 keV are due to the characteristic peaks in the 120 kVp spectrum.

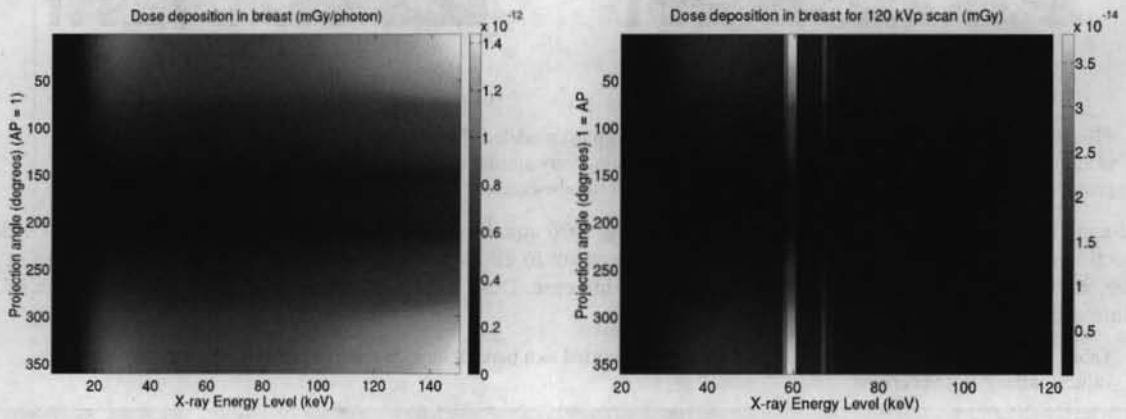

(a) (b)

Figure 3. (a) The normalized dose deposition matrix, $Q(\theta,E)$, quantifies dose in breast tissue (mGy/photon) for each energy level and projection angle of single CT rotation. Energy levels range from 5-150 keV in 1 keV increments, and projection angles range from 1-360 degrees in 1-degree increments. Other scan parameters are source-to-detector distance of 100 cm, source-to-isocenter distance of 50 cm, and detector z-extent of 16 cm. (b) The non-normalized dose-deposition matrix, $D(\theta,E)$, quantifies dose in breast tissue (mGy) for each energy level and projection angle of a specific scan protocol. The figure shown is the dose deposition matrix for a reference 120 kVp scan.

The dose deposition matrix for the shield simulation shows relatively lower dose deposited by energies in the range of 30-40 keV than in the reduced tube-current scan. (Figure 4). Nonetheless, these two protocols showed very similar dose reduction to the breast (shield: 23.42%, reduced tube current: 22.98%).

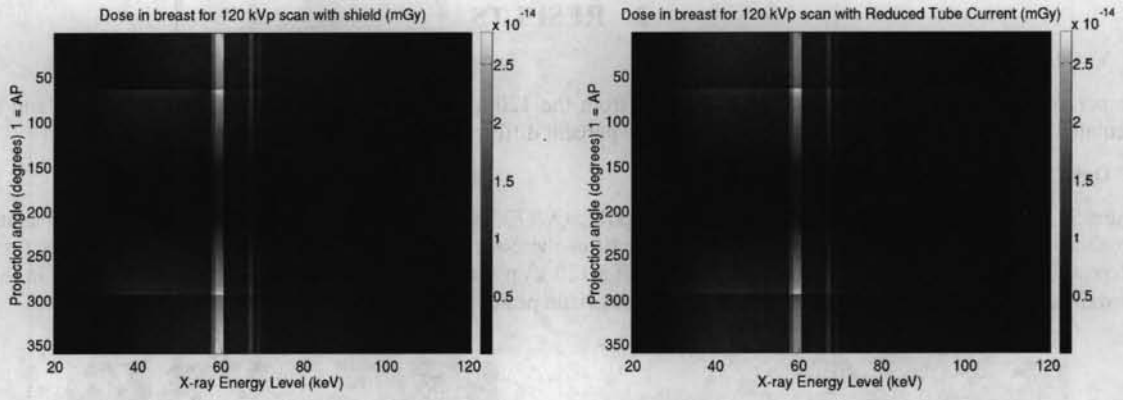

(a) (b)

Figure 4 Dose deposition matrices for a 120 kVp scan with (a) modeled shield and (b) reduced tube current for 130 AP-centered views. The matrices are nearly identical, indicating very similar dose deposition to breast across energy and projection angle for protocols utilizing a shield and reduced tube-current.

Reducing the input spectrum to 80 kVp and maintaining $N(\theta)$ equal to 1 as in the reference scan resulted in 2.37% dose reduction of dose to the breast. Reducing the input spectrum to 80 kVp while increasing $N(\theta)$ to match the dose at the detector of the 120 kVp scan resulted in 26.91% dose increase. Dose results are summarized in Table 1 for each of the simulated scans.

Table 1 Change in dose for different scan techniques, reported as a percent change relative to the reference scan. Negative values indicate dose decrease.

Scan Type	Spectrum (kVp)	N(θ)	Change in Dose (%)
Reference	120	1.00	-
Shield	120 [filtered] (130 AP views) 120 [non-filtered] (230 remaining views)	1.00	-23.42%
Reduced Tube Current (No Shield)	120	0.6065 (130 AP views) 1.00 (230 remaining views)	-22.98%
Reduced kVp	80	1.00	-2.37%
Reduced kVp	80	1.30	26.91%

4. DISCUSSION

Differences of 0.06% and 0.11% between the total dose values to breast reported from the 120 kVp and 80 kVp Monte Carlo simulations, respectively, and those calculated using Equation 2 with the same respective spectra suggest that our method of calculating total dose using a normalized dose deposition matrix is valid. This method is beneficial in that it allows investigation of numerous dose reduction techniques with various scan parameters (e.g. x-ray spectrum and mA) for a particular scan geometry without requiring additional computationally expensive Monte Carlo simulations for each protocol. As part of our future work, we plan to publish a database of dose deposition matrices for a variety of radiosensitive organs to enable researchers to study dose reduction methods and optimized techniques without requiring Monte Carlo simulations. Further, we plan to publish a $CTDI_{vol}$ dose deposition matrix, which will enable dose estimates for specific scanners and bowtie filtration.

Figure 3a demonstrates that high-energy photons deposit more dose per photon, despite being less likely to be absorbed. However, Figure 3b indicates that for a typical 120 kVp spectrum, low-energy photons contribute more dose than the high-energy photons, primarily because the spectrum contains more low-energy photons. This is especially apparent during AP-centered views, where the breast tissue is located closer to the source than in PA-centered views, and thus absorbs more low-energy photons.

Our results suggest that the dose deposited to the breast when using bismuth shielding is similar to that obtained by decreasing the photon fluence during AP views. Practically speaking, reducing the tube-current during the AP views to match the fluence exiting the shields has the same effect on dose deposition as using a spectrum that was filtered by a shield. Noise, contrast, and artifacts of the images resulting from these two protocols, however, will not necessarily be equal. Previous studies have demonstrated decreased image quality (increased noise and streak artifacts) due to shields and have suggested reduced mAs as an alternative.[17,18] One known issue with shields is that they incur an additional noise penalty during PA views by filtering out information-carrying photons that have exited the patient. Also, in practice, the shields are placed directly on the patient, and may deposit additional dose due to scattering photons.

When using the same number of emitted photons in the 80 kVp scan as the reference scan ($N(\theta)$ equal to 1), only a ~2% dose savings to the breast was observed. Moreover, when $N(\theta)$ for the 80 kVp scan was increased to 1.3 to match the dose at the detector of the reference scan (and thus expected noise variance of the images), there was an increase in dose of approximately 27%. These results suggest that eliminating high-energy photons from the spectrum without reducing the number of incident photons does not provide substantial dose savings to the breast. For this patient, reduction of dose to the breast with an 80 kVp spectrum would only be possible if the acquisition resulted in an improvement in image contrast such that the incident photon fluence could be reduced by at least 27%. The reduction in photon fluence required to reduce the dose is expected to depend on patient size.

Future work will expand upon these results by quantifying image quality of the dose reduction techniques described in this paper. The purpose of this study was to highlight the mechanisms by which dose is reduced in a few common dose reduction techniques in hope that a better understanding of these mechanisms will facilitate effective application and development of optimized dose reduction schemes.

5. CONCLUSION

Our results show that while both low- and high-energy photons deposit high levels of energy per emitted photon to the breast, low-energy photons deposit more dose to breast during a typical 120 kVp acquisition. Our results also demonstrate that dose deposited to the breast when using shields is similar to that obtained by decreasing the photon fluence during AP views. Dose reduction to the breast commonly observed in scans utilizing reduced kVp is caused by reduction in photon fluence rather than elimination of high- energy photons. Overall, results demonstrate that the factors affecting dose to the breast are complex, and a quantitative image quality assessment is required for complete analysis.

ACKNOWLEDGEMENTS

This project is funded in part by the US Food and Drug Administration, Office of Women's Health (OWH), and by the Oak Ridge Institute of Science and Engineering (ORISE). Performance of Monte Carlo simulations were made possible by NSF grant OCI-0923037.

REFERENCES

[1] "What's NEXT? Nationwide Evaluation of X-ray Trends: 2000 Computed Tomography." Conference of Radiation Control Program Directors, and Center for Devices of Radiological Health, United States Food and Drug Administration, Department of Health and Human Services, (2006).

[2] Brenner, D. J., and E. J. Hall. "Computed tomography--an increasing source of radiation exposure." New England Journal of Medicine 357(22), 2277-2284 (2007).

[3] "Health risks from exposure to low levels of ionizing radiation: BEIR VII Phase 2". Board on Radiation Effects Research, Division on Earth and Life Studies, Committee to Assess Health Risks from Exposure to Low Levels of Ionizing Radiation, National Research Council of the National Academies, Washington, D.C.: National Academies Press, (2006).

[4] Vollmar, S. V., and W. A. Kalender. "Reduction of dose to the female breast in thoracic CT: a comparison of standard-protocol, bismuth-shielded, partial and tube-current-modulated CT examinations." European Radiology 18(8), 1674-1682 (2008).

[5] Angel, E., et al. "Monte Carlo simulations to assess the effects of tube current modulation on breast dose for multidetector CT." Physics in medicine and biology 54(3), 497-512 (2009).

[6] Chang, K., W. Lee, D. Choo, C. Lee, and Y. Kim. "Dose reduction in CT using bismuth shielding: measurements and Monte Carlo simulations." Radiation Protection Dosimetry 138(4), 382-388 (2009).

[7] Coursey, C., D. P. Frush, T. Yoshizumi, G. Toncheva, G. Nguyen, and S. B. Greenberg. "Pediatric Chest MDCT Using Tube Current Modulation: Effect on Radiation Dose with Breast Shielding." American Journal of Roentgenology 190(1), W54-W61 (2008).

[8] Hurwitz, L. M., et al. "Radiation Dose Savings for Adult Pulmonary Embolus 64-MDCT Using Bismuth Breast Shields, Lower Peak Kilovoltage, and Automatic Tube Current Modulation." American Journal of Roentgenology 192(1), 244-253 (2009).

[9] Sempau, J., and Badal, A., "penEasy—A generic, modular main program and voxelised geometry package for PENELOPE," Code available at http://www.upc.es/inte/downloads/penEasy.htm

[10] penEasy Imaging, (2010). Code available at http://www.upc.edu/inte/en/descarregues.php.

[11] Salvat, F., Fernández-Varea, J. M., and Sempau, J., "PENELOPE-2006: A code system for Monte Carlo simulation of electron and photon transport." Proc., NEA-OECD, (2006). Code available at www.nea.fr/html/dbprog/peneloperef.html

[12] Christ, A., Kainz W., Hahn, E., et al. "The Virtual Family—development of surface-based anatomical models of two adults and two children for dosimetric simulations." Physics in Medicine and Biology. 55, N23 (2010).

[13] Hammerstein, G.R., D.W. Miller, D.R. White, M.E. Masterson, H.Q. Woodard, and J.S. Laughlin. "Absorbed radiation dose in mammography." Radiology 130(2), 485-491 (1979).

[14] "Publication 23: Report on the Task Group on Reference Man." International Commission on Radiological Protection, (1975).

[15] Woodard, H.Q., and D.R. White. "The composition of body tissues." British Journal of Radiology 59,(708), 1209-1219 (1986).

[16] Cranley, K., B. J. Gilmore, G. W. A. Fogarty, and L. Desponds. "Catalogue of Diagnostic X-Ray Spectra and Other Data." Report 78, Institute of Physics and Engineering in Medicine, (1997).

[17] Vollmar, S. V., and W. A. Kalender. "Reduction of dose to the female breast as a result of spectral optimisation for high-contrast thoracic CT imaging: a phantom study." The British journal of radiology 82(983), 920-929 (2009).

[18] Geleijns, J., M Salvado Artells, W. J. H. Veldkamp, M. Lopez Tortosa, and A. Calzado Cantera. "Quantitative assessment of selective in-plane shielding of tissues in computed tomography through evaluation of absorbed dose and image quality." European Radiology 16(10), 2334-2340 (2006).